Nonviral Gene Delivery Vectors Use Syndecan-Dependent Transport Mechanisms in Filopodia To Reach the Cell Surface

Zia ur Rehman, Klaas A. Sjollema, Jeroen Kuipers, Dick Hoekstra, and Inge S. Zuhorn*

University Medical Center Groningen, University of Groningen, Department of Cell Biology, A. Deusinglaan 1, 9713 AV Groningen, The Netherlands

ABSTRACT

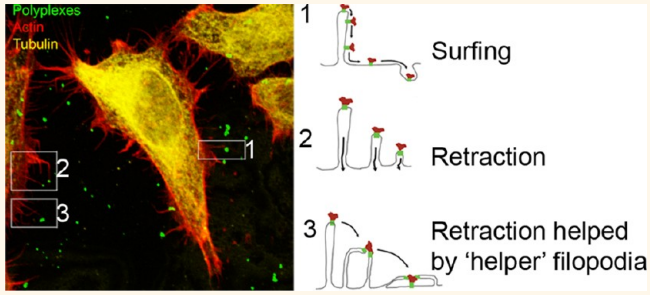

Lipoplexes and polyplexes, that is, assemblies of cationic lipids and polymers with nucleic acids, respectively, are popular nanocarriers for delivery of genes or siRNA into cells for therapeutic or cell biological purposes. Although endocytosis represents a major mechanism for their cellular entry, very little is known about parameters that govern early events in the initial interaction of such delivery devices with the cell surface. Here, we demonstrate that prior to entry, poly- and lipoplexes are captured by thin, actin-rich filopodial extensions, protruding from the cell surface. Subsequent additional recruitment and local clustering of filopodia-localized syndecans, presumably driven by multivalent interactions with the polycationic nanocarriers, appear instrumental in their processing to the cell body. Detailed microscopic analyses reveal that the latter relies on either directional surfing along or retraction of the filopodia. By interfering with actin polymerization or inhibiting the motor protein myosin II, localized at the base of filopodia, our data reveal that the binding of the nanocarriers to and subsequent clustering of syndecans initiates actin retrograde flow, which moves the syndecan-bound nanocarriers to the cell body. At the present experimental conditions, inhibition of this process inhibits nanocarrier-mediated transfection by 50—90%. The present findings add novel insight to our understanding of the mechanism of nanocarrier-cell surface interaction, which may be instrumental in further improving delivery efficiency. In addition, the current experimental approach may also be of relevance to improving our understanding of cellular infection by viruses and pathogenic bacteria, given a striking parallel in filopodia-mediated processing of these infectious particles and nanocarriers.

KEYWORDS: lipo/polyplexes · polycationic nanocarriers · filopodial extensions · actin retrograde flow

Transfection involves the cellular introduction of nucleic acids, including plasmids for gene expression, and oligonucleotides such as antisense RNA or siRNA for regulating protein expression. Accordingly, it is a versatile approach in cell biology, for example in studies of protein function, and holds promise for future therapeutics, like in gene therapy and cancer. Both viral and nonviral delivery systems have been applied for that purpose, each displaying distinct advantages and disadvantages.[1] Nonviral delivery systems are commonly based on the application of cationic lipids or polymers which together with DNA or RNA spontaneously assemble into so-called lipo- or polyplexes, respectively. For effective transfection to occur, both types of complexes require a net positive charge and, accordingly, it is generally believed that electrostatic interactions are relevant in the early interactions of either complex with the highly negatively charged cell surface.[2−4] Subsequently, the cationic vectors are internalized by means of endocytosis, and the precise route of internalization, that is, clathrin-, caveolae-, and nonraft-mediated endocytosis, macropinocytosis, or a combination of these pathways, may depend on parameters like cell-type, and nature and size of the vectors.[5−8] Although these entry pathways have been extensively characterized in recent years, very little is known about how nanocarriers initially interact with the cell surface, which may harbor an intricate network of macromolecules, including proteins and polysaccharides, assembled into an organized meshwork. As such this meshwork may constitute a potential barrier for nanocarriers prior to reaching the cell body, where endocytic internalization subsequently occurs, while at the same time it may provide the cellular receptors for nanocarrier binding. We have previously shown that non-targeted lipoplexes exploit β-integrin receptors for productive transfection entry in polarized MDCK cells.[9] Similarly, liposomes, lipoplexes, and polyplexes have been shown to use transmembrane heparan sulfate proteoglycans (HSPGs) as receptors.[10,11] The involvement of a specific class of HSPGs, that is,

* Address correspondence to i.zuhorn@umcg.nl.

Received for review June 27, 2012 and accepted August 2, 2012.

Published online August 02, 2012
10.1021/nn3028562

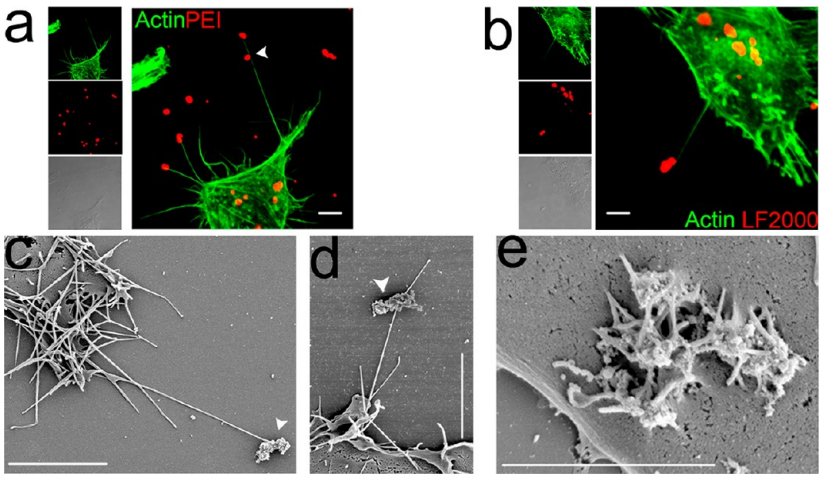

Figure 1. Poly- and lipoplexes attach to filopodia prior to cellular entry *via* endocytosis. HeLa cells, plated on glass coverslips 1 day before the experiment, were incubated with polyplexes (a and c−e) or lipoplexes (b) at 37 °C. After 90 min, the cells were fixed and processed for either confocal microscopy (a,b) or scanning electron micoscopy (c−e). For visualization of poly- and lipoplexes by confocal microscope the complexes contained Cy3-labeled plasmid DNA. Filopodia were visualized by staining with alexa-488-labeled phalloidin. Arrow heads (a, c, and d) indicate the binding of polyplexes to the filopodia. Scale bars are 5 μm (a−d) and 3 μm (e).

syndecans, was originally suggested by Behr and co-workers.[10] Interestingly, HSPGs have also been shown to act as (co)receptor for both viruses, including papillomavirus, herpes virus, adenovirus, retrovirus and flavivirus,[12−15] and bacteria.[16,17] Moreover, a potential role of syndecans has been suggested in the surfing of viruses along thin, actin-rich cellular extensions, known as filopodia,[18] representing a mechanism preceding the actual entry of viruses into cells.[19]

These considerations have prompted us to investigate early events in the interaction of PEI polyplexes and Lipofectamine lipoplexes with the surface of HeLa cells in order to clarify the overall mechanism of their cellular entry. Previously,[8] we demonstrated that both caveolae- and clathrin-mediated endocytosis are involved in the entry of such nanocarriers into HeLa cells. However, except for a potential involvement of syndecans in this entry process,[20] little is known about the actual mechanism underlying this involvement or whether filopodia, like in viral and bacterial entry, could play a role. Here, we demonstrate that prior to entry; lipo- and polyplexes are captured by thin, actin-rich filopodial extensions, protruding from the cell surface. Subsequent oligo(poly)merization of syndecans appears instrumental in the processing of nanocarriers along and *via* these extensions to the cell body, prior to actual endocytic entry into the cell.

RESULTS AND DISCUSSION

Poly- and Lipoplexes Attach to Filopodia Prior to Cellular Entry *via* Endocytosis. Nucleic acid-containing nanocarriers, such as lipoplexes and polyplexes, deliver their cargo into cells after internalization *via* endocytosis, including clathrin-, caveolae-mediated endocytosis, and macropinocytosis. Yet, very little is known about steps preceding actual internalization of nanocarriers into cells. However, the presence of dynamic actin-rich protrusions on the cell surface, including filopodia, retraction fibers and microvilli,[21] has been well established. Moreover, since both distinct viruses[18,19,22,23] and bacteria[24] exploit such surface extensions to acquire access to the cell body prior to cellular entry, we wondered whether nanocarriers could use a similar route, prior to their endocytic entry into the cell. To this end, we first examined the interaction of PEI polyplexes and Lipofectamine lipoplexes at the surface of HeLa cells by confocal microscopy. As shown in Figure 1, numerous actin-rich protrusions, presumably reflecting filopodia and retraction fibers, extend from the cell surface into the extracellular environment, and serve s attachment sites for fluorescently tagged (red) PEI polyplexes (Figure 1a) and Lipofectamine lipoplexes (Figure 1b) Analysis by scanning electron microscopy showed that the length of the filopodia, which were mostly straight and nonbranched structures, varied from 5 to 20 μm, with diameters of 50−200 nm (Figure 1c). Apart from binding to the tips, emphasizing the sensory role of filopodia in probing the extracellular environment, polyplexes were also found to localize along the protrusions (cf. arrow heads in Figure 1a,d) and in cases attachment of more than one polyplex to a filopodial extension was noted (Figure 1a). Furthermore, poly- or lipoplexes attached to the cell body were also frequently surrounded by several filopodia (Figure 1e), implicating a potential correlation between the latter structures and cell body localization of the nanoparticles. Importantly, very similar observations were made in other cell lines, including hCMEC/D3 human cerebral microvascular endothelial cells, HEK 293 cells, and PC3 cells, a prostate cancer cell line (Supporting Information Figure S1).

Thus these observations indicated a potentially active role of filopodia in the early recruitment of

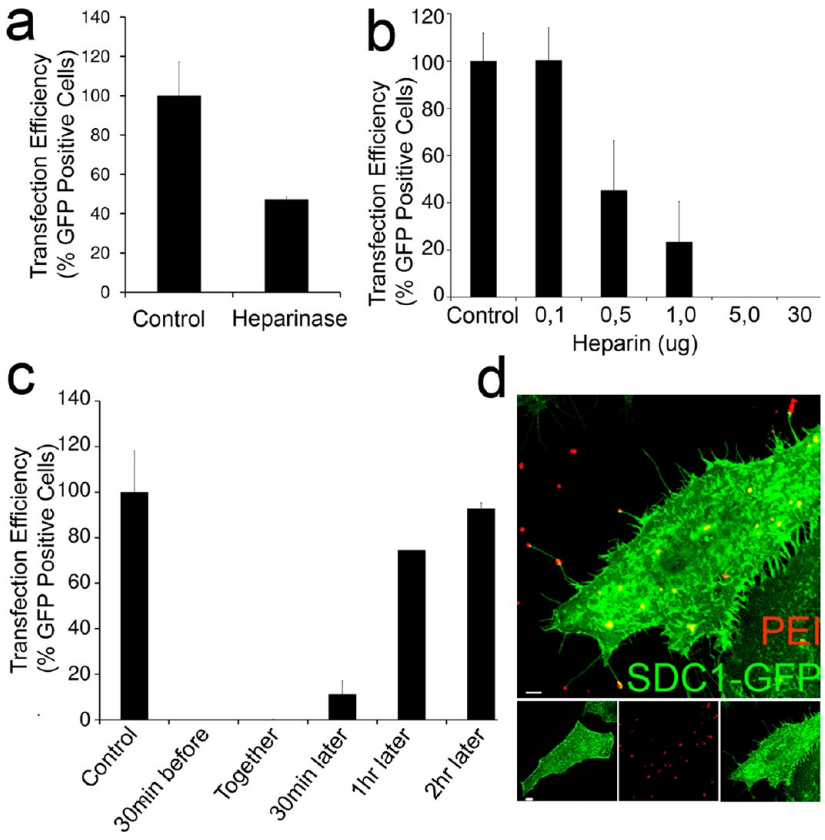

Figure 2. Heparan sulfate proteoglycans, in particular syndecans, are involved in the binding of poly- and lipoplexes to filopodia. (a) To remove cell surface heparan sulfate the HeLa cells were treated with heparinase for 30 min, followed by addition of the polyplexes with heparinase still present. After an incubation for 2 h at 37 °C, the cells were washed and incubated in complete medium. After 48 h the transfection efficiency (mean ± SEM, $n = 6$) was measured as described in Materials and Methods. (b, c) Heparin (5 μg/mL), preincubated with the cells for 30 min prior to addition of the polyplexes (2 h at 37 °C) competitively inhibited polyplex-mediated transfection efficiency (determined after 48 h; mean ± SEM, $n = 6$) in a concentration (b) and time (c) dependent manner. (d) HeLa cells expressing syndecan-1 tagged with GFP (SDC1-GFP) were incubated with polyplexes for 90 min, and subsequently fixed and mounted on a glass slide for examination by confocal microscopy. Note the colocalization of polyplexes and syndecan-1, reflected by yellow fluorescence. The lower middle and right square show the individual image channels. The lower left square shows a syndecan-1-expressing cell without polyplexes. Scale bar, 3 μm.

cationic poly- and lipoplexes by cells. In addition, we took into account a potential role of cell surface polyanionic heparan sulfate proteoglycans (HSPGs), such as syndecans, which have been shown to be involved in the internalization process of liposomes and positively charged poly- and lipoplexes.[10,11,20,25] To this end HeLa cells were treated with heparinase to remove heparan sulfate[26] prior to the addition of PEI polyplexes. As shown in Figure 2a, PEI-mediated transfection efficiency was inhibited by approximately 50% following heparinase pretreatment. Consistently, treatment of the cells with sodium chlorate, which inhibits the sulfation of HSPGs, reduced the internalization of fluorescently labeled PEI polyplexes (approximately 50%; not shown). Also the addition of heparin, which competes with the HSPGs for polyplex binding,[25,27] inhibited polyplex uptake and subsequently PEI-mediated transfection in a concentration- (Figure 2b) and time- (Figure 2c) dependent manner. The competitive effect of heparin is apparent when the compound is added not later than 30−60 min after addition of the polyplexes, which coincides with the kinetics of actual internalization of the nanocarriers by the cells (not shown, *cf.* ref 8). Together these data suggest that filopodia, in conjunction with proteoglycans, play a pivotal role in cellular binding and processing of PEI polyplexes and Lipofectamine lipoplexes in cell transfection. Except for some quantitative differences, the processing of the polyplexes appeared very similar as that of lipoplexes. To further reveal mechanistic details of this process, in the following we therefore will largely focus on data obtained with PEI polyplexes; where relevant, a reference will be made to Lipofectamine lipoplexes.

Particularly syndecans, as major representatives of the HSPG family, have been recognized as key players in the entry of viruses[15] as well as polyplexes.[20] To visualize this interaction, we therefore expressed GFP-labeled syndecan-1 (SDC1-GFP) in HeLa cells, as described in Materials and Methods, which were subsequently incubated with fluorescently labeled polyplexes. As shown in Figure 2d, SDC1 is homogeneously distributed over the entire cell surface of HeLa cells, whereas upon addition of

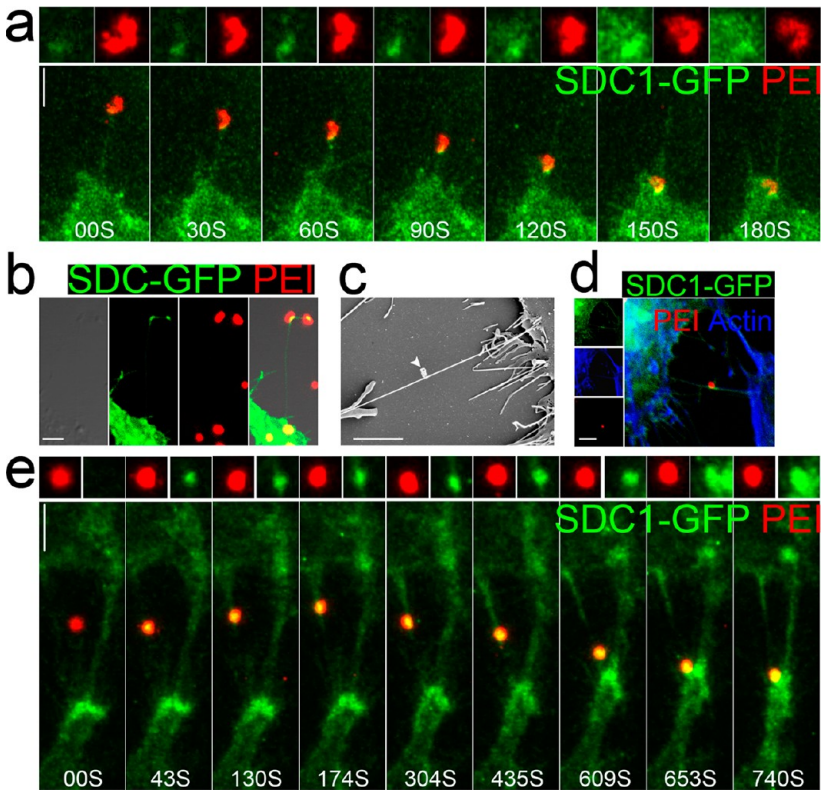

Figure 3. PEI polyplexes surf along filopodia to reach cell body. (a) HeLa cells expressing SDC1-GFP (green) were incubated with polyplexes with cy3-labeled plasmid DNA (red) and polyplex-cell interaction was visualized by time-lapse microscopy. Selected frames from Supporting Information movie 1 reveal the surfing of polyplexes along syndecan-rich filopodia. The upper row of frames shows fluorescence images of the polyplex and the local presence of syndecan-GFP fluorescence at the polyplex binding site to the filopodium, indicating a rapid recruitment of syndecans (time intervals are in seconds) to the binding site of polyplexes. (b) Syndecan clustering (green channel) is prominently present at polyplex-binding sites along filopodia (c). Next to filopodia, polyplexes also bind to nanotubes (arrowhead), connecting two cells. (d) Nanotubes were stained with alexa 633 labeled phalloidin, revealing the actin-rich structures (pseudocolored blue) to which polyplexes (red) bind, and displaying clustered SDC1-GFP (green) at the binding site of polyplexes (compare green *versus* red channel, left pannels in d). (e) Selected frames (after time intervals (seconds) as indicated) from Supporting Information movie 2, showing time lapse microscopic images of polyplexes (red) interacting with nanotubes between HeLa cells, expressing SDC1-GFP (green). Note the rapid recruitment of syndecans at the binding site of the polyplexes (upper panel in e), and the dynamics of polyplex movement. Initially (frame 2−4) the nanocarriers move upward, followed by a reversed movement (frame 5 and following) toward the surface of the opposite cell. Scale bar is 3 μm.

polyplexes it organizes in clusters. As anticipated, based on the inhibition experiments described in the previous paragraph (Figure 2a−c), a substantial colocalization was seen between syndecans and polyplexes, their close interaction being reflected by a yellow (green + red) signal. Possibly, the yellow spots in the plane of the cell body surface are derived from clusters of polyplexes and filopodia, like those shown in Figure 1e. Certainly, the involvement of SDC1 in the tight binding of polyplexes to the filopodia is most clearly discerned in those protruding from the cell body. A similar colocalization, was seen in cells expressing RFP-syndecan-2 (SDC2-RFP) (not shown), implying that both types of proteoglycans are actively involved in binding PEI polyplexes to the filopodia.

Evidently, attached polyplexes do not enter cells at the filopodia (Figure 1; *cf.* refs 22, 24, and 28). Rather, once attached, the polyplexes presumably exploit these cellular protrusions to reach the plasma membrane surface at the cell body for entry into the cell. We therefore focused next on the mechanism as to how filopodia-attached PEI polyplexes reach the cell body.

PEI Polyplexes Reach the Cell Body by Surfing along Filopodia. To gain insight into the potential processing of polyplexes along filopodia, including the role of syndecans, PEI polyplexes were prepared containing fluorescently labeled DNA, as described in Materials and Methods. Movement of the polyplexes along the filopodia was then directly visualized by live cell imaging in HeLa cells, expressing SDC1-GFP. As shown in Figure 3a and Supporting Information Movie 1, following binding, the polyplexes surf along the filopodia to the surface of the cell body. Simultaneously, the intensity of the syndecan fluorescence increases at the binding site between polyplex and filopodia (Figure 3a, upper panel), suggesting the participation of syndecan 1 in this process, as further supported by an increase in the colocalization signal. Further support for this notion is shown in Figure 3b, where attachment of two polyplexes to a filopodial extension highlight an intimate interaction between seemingly clustered syndecans and the cy3-labeled polyplexes at the site of attachment. Furthermore, as is apparent from Figure 3a and

Movie 1, when polyplexes are attached, the filopodia does not zipper around the nanocarrier, that is, while the cell body-directed movement of the nanocarrier is progressing, the protrusion itself remains extended into the extracellular environment. Accordingly, together these data fit a mechanism that is very reminiscent of that in which EGF receptors have been shown to undergo a retrograde flow along filopodia after binding EGF.[28] Thus, in a similar fashion, recruitment and clustering of negatively charged syndecans can occur, triggered by the multivalency of the interacting positively charged polyplex, thereby presumably providing the driving force for cell surface directed transport along the filopodia (see further below).

Interestingly, in passing we also noted that polyplexes can travel along actin-rich tubes, which connect adjacent cells (Figure 3c–e). Such tubes are defined as "nanotubes"[29] and can be as long as 100 μm. These structures gained considerable interest because of their potential role in facilitating intercellular transport of organelles, vesicles, and membrane bound proteins.[29–31] Furthermore, also intercellular transport of viruses through these nanotubes from an infected to uninfected cell,[32,33] their surfing along the surface of nanotubes,[34] as well as that of bacteria between macrophages[31] has been reported. However, underlying mechanisms have been only poorly addressed. As shown in Figure 3e and Supporting Information Movie 2, fluorescently labeled PEI polyplexes also attach to the surface of such nanotubes, which are seen between HeLa cells and express GFP-labeled syndecan1. Scanning electron microscopy supports the notion that polyplexes bind to the surface of such nanotubes (Figure 3c, arrowhead). After initial binding of the polyplexes to the actin-rich nanotube (Figure 3d), the syndecan receptors are rapidly recruited to the binding site, as reflected by a rapid local increase of GFP fluorescence and strong increase in colocalization signal at the polyplex binding site (Figure 3d,e, upper panel), which largely occurs prior to their lateral movement (movie 2). Intriguingly, rather than moving unidirectionally, as observed following attachment to filopodia, polyplexes bound to the nanotubes can, at least in part, move in either direction of the nanotube, connecting the two cells. Thus, after initially moving in one direction (Figure 3e, frames 1–4), transport of the polyplex subsequently changed directions and reached the surface of the opposite cell (Figure 3e, frames 5–9). This bidirectional movement along intercellular nanotubes could take its origin in the formation of actin tension fibers (see below) or reciprocal movements of a partially syndecan-neutralized polyplex being attracted by approaching cell body-produced syndecans, by both cells.

Altogether, these observations demonstrated that polyplexes can surf along filopodia and nanotubes to the cell body, while oligomerization or polymerization of syndecans appears a commensurating event.

Evidently, so far our data show that filopodia and intercellular nanotubes provide a cellular road for the trafficking of nanocarriers, traveling with a rate of 0.3–3 μm/min, on their way to the surface of the cell body for cellular entry. However, we also noted that next to surfing along a filopodia, several protrusions on the cell surface may display a concerted dynamic behavior involving their retraction, as a consequence of which the nanocarrier may also reach the cell body.

Retraction of Filopodia Transfers Polyplexes to the Cell Surface. Retraction of filopodia has been noted, based on observations that "short-lived" filopodia capture viruses, which are localized near the cell surface[23]. Similarly, bacteria can also be actively retracted by filopodial extensions to bring them to the cell body.[24] Next to surfing along filopodia and nanotubes, this mechanism of retraction also appears to contribute to carrying polyplexes to the cell body, presumably preceding their actual internalization (Figure 4a, Supporting Information Movie 3). Thus after initial binding of fluorescent PEI complexes to the filopodia of GFP-syndecan expressing HeLa cells, extensive clustering of syndecans is seen to occur (Figure 4a, top panel, green channel) at the binding site of the PEI nanocarriers, as also reflected by the immediate increase in colocalization signal between GFP and CY3. Interestingly, as a subsequent process, rather than surfing along the protruding filopodia, the protrusions shorten, which likely reflects the process of retraction, while the nanocarriers remain attached to the top of the rapidly collapsing filopodia. This process may occur as such. However, when in addition adjacent filopodia or fibers are within reach of the "incoming" nanoparticle, they may also attach to the nanocarrier, thus apparently assisting as "helper" filopodia in the homing process toward the cell body (Figure 4a, fourth panel arrowhead). Indeed, as shown in Figure 4b (and Supporting Information movie 4), although multiple filopodia/fibers, particularly near the cell body, could be involved, initial attachment to one (arrowhead 1, second panel Figure 4b) followed by its early retraction, prior to attachment of several others (Figure 4b, arrowhead 2, third panel, and arrow heads 3 and 4, fourth panel) that might assist in cell body directed transfer, seems to be the scenario for this transport process. The simultaneous attachment of several (extended) filopodia to one nanoparticle was often observed, as revealed by fluorescence (Figure 4c) and scanning electron microscopy (Figure 4d).

To summarize, nanocarriers can be transferred to the cell body by different mechanisms, including surfing along extended protrusions or *via* retraction after initial attachment, during which syndecan receptors are recruited to the binding site.

Filopodia Sense PEI Complexes in the Extracellular Environment. Filopodia are generally considered as the antennae of the cell, "probing" the extracellular environment.

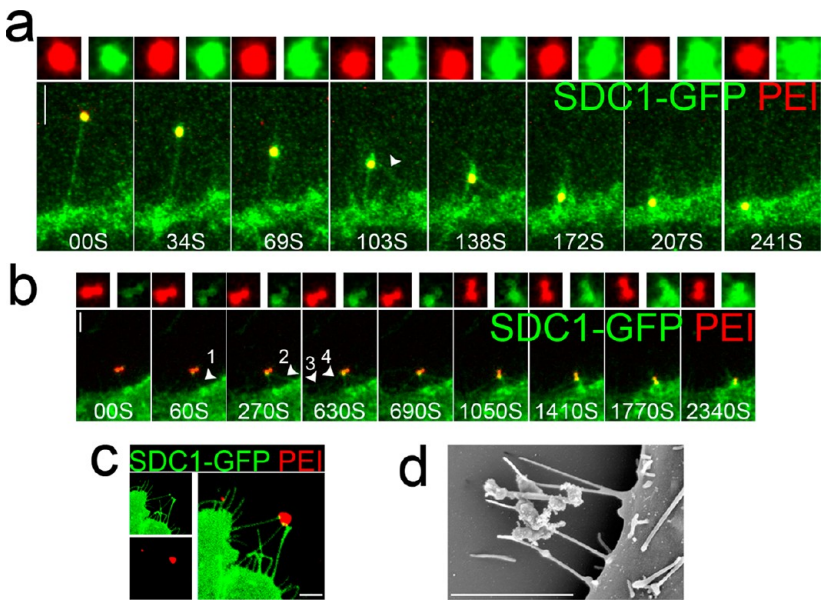

Figure 4. Retraction of surface protrusion as an alternative mechanisms for polyplex transfer to the cell surface (a) Cells, expressing SDC1-GFP (green), were incubated with polyplexes labeled with cy3-tagged plasmid DNA (red) and the interaction was monitored by time-lapse microscopy. Frames were selected from Supporting Information movie 3 showing that after binding to filopodia, syndecans are recruited to the binding site of the polyplexes, after which the filopodia retract thereby concomitantly transferring the attached polyplex to the cell surface. Adjacent filopodia may assist in this process (frame 4, arrowhead). The images above the frames reflect the increased recruitment of syndecans (green), as a function of time (secs), near the filopodia-bound polyplexes (red), their colocalization showing as yellow in the frames. (b) Selected frames from Supporting Information movie 4, showing that initially one filopodium binds to the polyplex (arrowhead 1, frame 2). Subsequently, adjacent filopodia (arrowheads 2, 3, and 4), and further highlighted in panels c (confocal image) and d (scanning electron microscopy), may assist in the ultimate translocation of the polyplex to the cell surface. Scale bar, 3 μm.

Distinct receptors that can trigger certain signaling processes are involved in this sensing process, which respond to the gradient of ligands or chemo-attractants over a certain distance.[21,35] How filopodia respond to an individual ligand has not been studied in detail.

When HeLa cells, expressing SDC1-GFP, were incubated with PEI-Cy3-labeled polyplexes, time-lapse microscopy analysis revealed that filopodia actively extend toward polyplexes, prior to directly interacting with the nanocarrier, thus reflecting their sensing ability (Supporting Information movie 5a, Figure 5a). The latter is apparent from the red appearance of the nanoparticle, which upon direct interaction with the SDC1-GFP labeled filopodium reveals a (local) yellow signal, as a result of colocalization between Cy3 and GFP. Separate visualization of the GFP fluorescence (blue channel, Figure 5a, upper panel) suggests that a rapid clustering of syndecans takes place at the filopodium tip upon contacting the polyplex (Figure 5a, upper panel, frames 5 and 6). After attachment and recruitment and apparent oligomerization of syndecans (Figure 5a, frame 5) the nanocarrier commences to surf along the filopodium toward the cell body (Figure 5a, frames 5−9).

Strikingly, the formation of a u-turn by the filopodium prior to the attachment of a polyplex (Supporting Information movie 5b), supports an apparent sensing of the presence of polyplexes by filopodia. The dynamic behavior, as opposed to a static protrusion extending into the extracellular environment, is further supported by the observation in Figure 5b, showing a perpendicularly bended filopodium, with two attached PEI polyplexes, clearly revealing the strongly clustered syndecans, highlighted by spots of intense green fluorescence at the sites of attachment (Figure 5b, left image, middle panel). Evidently, several nanocarriers can attach and surf simultaneously along the same filopodia (Figure 5c, arrow heads) and several filopodia which are near one nanoparticle may sense its presence and establish multiple contacts (Figure 5c, arrow). Not surprisingly, as revealed by scanning EM (Figure 5d) and confocal microscopy (Figure 5e), filopodia on a given cell may even sense nanoparticles that are attached to (filopodia of) adjacent cells. In that sense, the presence of the nanoparticles triggers very similar cell biological responses as has been reported for cell surface-attached viruses[22] in that intercellular filopodial bridges are formed, allowing intercellular trafficking.

The data as presented so far clearly indicate a role of syndecan in nanocarrier binding, while its dynamics, as part of the retrograde transport machinery, possibly represents a driving force for the surfing of polyplexes along the filopodia. Specifically, after initial attachment, recruitment and oligomerization of syndecans seem a prerequisite for surfing of poly- and lipoplexes along filopodia in order to reach the cell body. To obtain further experimental support for this notion, the next experiments were carried out.

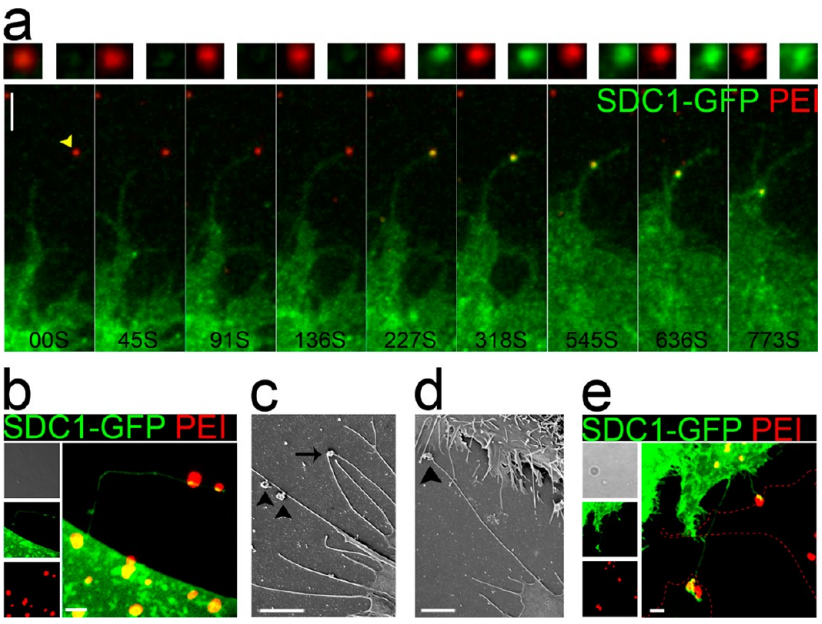

Figure 5. Filopodia sense PEI complexes in the extracellular environment. (a) Selected frames from Supporting Information movie 5a showing that filopodia are extending toward polyplexes, prior to their attachment. SDC1-GFP (green) expressing HeLa cells were incubated with polyplexes (red) and monitored by time-lapse microscopy. As reflected by the fluorescence images above the frames, a distinct attachment of the nanocarrier (red) becomes apparent after approximately 140 s, when colocalization of syndecan and polyplex (appearance of green fluorescence (syndecan) at the polyplex binding site, images at 136 *vs* 227 s) becomes apparent (yellow fluorescence in the corresponding frames). (b) HeLa cells, expressing SDC1-GFP, were incubated with polyplexes for 90 min and subsequently examined by confocal microscopy, showing a filopodium perpendicularly bending toward polyplexes and a concomitant clustering of syndecan-1 at the binding sites of the polyplexes. (c) Scanning electron micrograph of HeLa cells incubated with polyplexes showing that several polyplexes can surf along the same filopodium (arrow heads), and that several filopodia may sense the same polyplex (arrow). (d,e) Scanning electron microscopy of HeLa cells (d) and confocal images of HeLa cells expressing SDC1-GFP (e), incubated with polyplexes for 90 min, showing that filopodia can also bind to the polyplexes that are already attached to a neighboring cell, thereby forming filopodial bridges. See text for details. Scale bar, 3 μm.

Syndecan-Actin Interactions Determine Polyplex Trafficking along Filopodia. Syndecans are transmembrane proteins that interact with the actin cytoskeleton *via* their intracellular domains that interact with PDZ-containing proteins. Accordingly, analogously as reported for viruses and bacteria,[36] the dynamics of nanocarrier–surface interactions and the eventual fate of the surface attached nanocarrier is presumably dictated by coordinated syndecan–actin interactions. To obtain mechanistic support for this notion, we therefore investigated the extent to which actin dynamics affected filopodia-mediated processing of the polyplexes. Actin retrograde flow, which involves a net transport of actin molecules from the plus end at the tip of an actin protrusion toward the minus end at the cell body, appears a key event in this mechanism. In essence, three basic processes contribute to this mechanism, that is, (i) actin polymerization at the tip of the filopodia, (ii) depolymerization of the actin filaments, and (iii) a pulling mechanism exerted by the anchored motor protein myosin II, localized at the base of filopodia and also present in retraction fibers.[18,37,38] A perturbation in any of these three steps will frustrate filament dynamics, and therefore likely halt filopodia- and retraction fiber-mediated translocation of the polyplexes. To investigate this, we started out with treating the cells with blebbistatin, a specific myosin II inhibitor.[39] After pretreating the cells with the inhibitor (50 μM, *cf.* Figure 7) for 30 min after which the polyplexes were added, still in the presence of the inhibitor, transfer of attached polyplexes to the cell surface was completely inhibited (Figure 6a, Supporting Information Movie 6). Intriguingly, careful examination indicates that upon initial interaction, some recruitment of syndecans to the binding site is triggered, although to a lesser degree than at control conditions, as reflected by a lower level of GFP fluorescence intensity at the polyplex binding site, proportionate with a significant diminishment in the colocalization signal (*cf.* Figures 3a and 4a *versus* 6a). In fact, the recruitment of syndecans appears transient, and concomitantly the "tightness" of the polyplex–syndecan interaction presumably weakens, as indicated by the subsequent decrease in the GFP-Cy3 colocalization signal at the attachment site (Figure 6a, upper panel, frames 6–8) . These data thus suggest that long-term stable multivalent interactions between syndecans and polyplexes do not seem to form without a further "in-flow" of additional syndecans, as apparently arises when retrograde F actin flow is blocked. Rather, at these conditions, the syndecan receptor-density at the binding site decreases and, accordingly, the binding strength of the polyplexes to filopodia likely weakens.

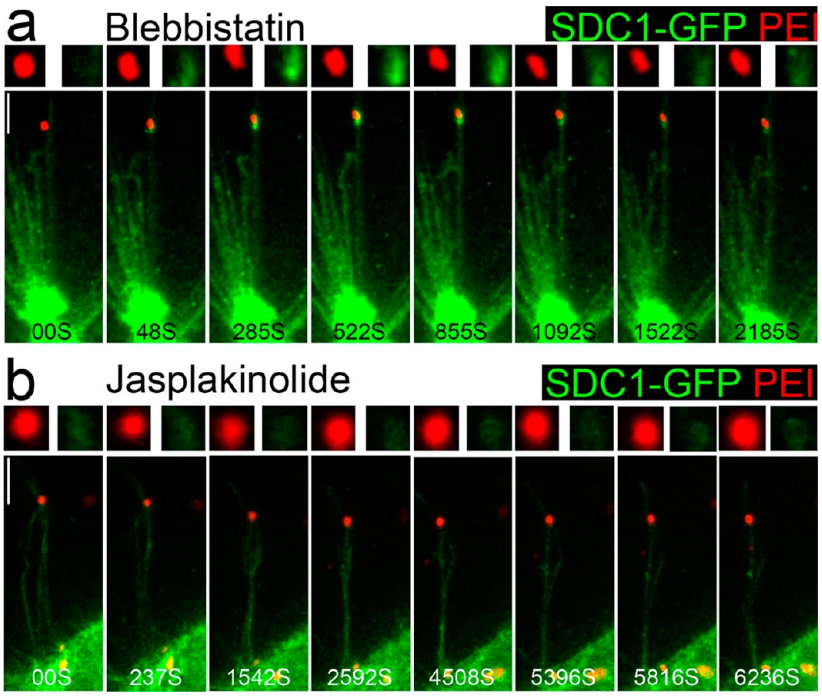

Figure 6. Syndecan–actin interactions determine polyplex trafficking along filopodia. (a) HeLa cells, expressing SDC1-GFP (green), were pretreated with 50uM blebbistatin (myosin II inhibitor) for 30 minutes. Subsequently, cy3-labeled polyplexes (red) were added and visualized by time-lapse microscopy. Selected frames from Supporting Information movie 6 demonstrate that after initial binding to the filopodium, the polyplex recruits syndecan-1 to its binding site, but the following steps (retraction or surfing) are impeded. The upper row of images above each frame shows the fluorescence of polyplex and syndecan at the binding site. Note the transient recruitment of syndecan, reflected by a relative fading of the green fluorescence and the disappearance of yellow fluorescence (after approximately 855 s). (b) Selected frames from Supporting Information movie 7b showing that the actin stabilizer jasplakinolide (100 nM, 30 min treatment prior to addition of the polyplexes) inhibits the lateral movement of syndecans, as apparent in SDC1-GFP expressing cells, to the binding site of polyplexes (upper row, compare Figure 6a). Simultaneously, transport of polyplexes to the cell body is completely inhibited. Scale bar is 3 μm.

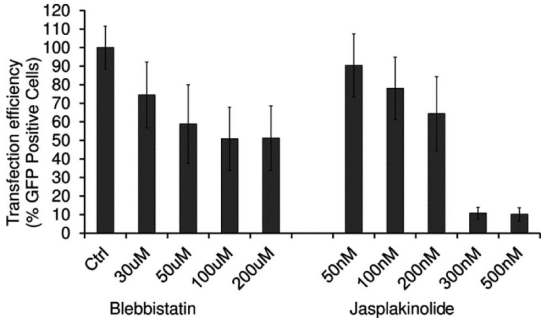

Figure 7. Filopodia-mediated transport of polyplexes contributes prominently to overall transfection efficiency. HeLa cells were pretreated with the indicated concentrations of either blebbistatin or jasplakinolide for 30 min, followed by the addition of polyplexes, containing a GFP-expressing reporter gene. After 2 h, the cells were washed and further incubated in complete medium, without blebbistatin or jasplakinolide and polyplexes. After 48 h, the transfection efficiency was determined by measuring the percentage of cells expressing the reporter gene (mean ± SEM, n = 6).

Apart from a complete immobilization, it is therefore possible, that the nanocarriers eventually dissociate from the filopodia, and hence from the cells, thereby frustrating transfection efficiency (see below).

In line with the foregoing, affecting the state of actin polymerization similarly strongly interfered with filopodia-mediated processing of the polyplexes. Thus preincubation of the cells with cytochalasin D, a reagent that binds to the barbed end of actin filaments, thereby preventing its polymerization and causing subsequent depolymerization, also abrogated polyplexes transport along the filopodia (not shown).

Finally, addition of jasplakinolide, which stabilizes actin filaments and hence induces polymerization, also strongly inhibited the movement of attached polyplexes toward the cell body (Figure 6b, Supporting Information Movie 7a). In this case, significant recruitment of syndecan receptors to the polyplex was not observed, as reflected by only minor changes in GFP-fluorescence intensity (Figure 6b, top panel), reflecting the local density of the syndecan receptors, localizing at the polyplex binding site. Moreover, the absence of a visible colocalization signal further indicated the relative weakness of the syndecan–polyplex binding. Our data are therefore entirely consistent with previous observations that stabilization of actin filaments by jasplakinolide inhibits the lateral movement of receptors, and hence receptor clustering.[40] Receptor oligomerization has been shown to be necessary for downstream signaling and subsequent retrograde transport of receptor–ligand complex.[28] Additionally,

in line with the notion mentioned above that a diminished ability of syndecan recruitment may weaken polyplex binding to filopodia, and eventually their dissociation from the cells, we indeed observed in cells treated with jasplakinolide that polyplexes detached from filopodia following initial attachment (Supporting Information movie 7b). In addition in cells treated with jasplakinolide polyplexes sometimes move away from the cell body showing `reverse surfing' (Supporting Information movie 7c). This shows that interaction of polyplexes to the cell surface is not a simple electrostatic interaction, instead it is under tight regulation of cellular processes.

Together, our data indicate that nanocarriers, similarly as noted for viruses, exploit filopodia to acquire access to the cell body *via* an actin- and motor-driven process. Actin-interacting syndecan appears instrumental in this process, showing that after attachment the protein's density locally increases at the poplyplex attachment site, as reflected by a local increase in GFP fluorescence and a strong colocalization signal. Interference with these events immobilizes the particles and eventually may cause their dissociation from the cells. Thus syndecan recruitment and clustering (oligomerization and/or polymerization), which depends on an intact actin filament system, appears a prerequisite for syndecan-polyplex directionality of retrograde transport along filopodia.

Filopodia-Mediated Transport of Polyplexes Contributes Prominently to Overall Transfection Efficiency. Thus far the data demonstrate that cell surface protrusions are closely involved in "capturing" polyplexes that subsequently acquire access to the cell body by means of either a syndecan-mediated surfing or a retraction mechanism along filopodia and retraction fibers. It was however, of obvious interest to determine whether these mechanisms actually lead to transfection, that is, cellular internalization of the polyplexes and, if so, what their relative contribution might be to overall transfection efficiency. We therefore analyzed the effect of jasplakinolide and blebbistatin, both of which strongly impede filopodia-mediated transport, on the transfection efficiency of PEI polyplexes.

To this end, the cells were preincubated with either inhibitor for 30 min, followed by addition of the polyplexes, while keeping the selected inhibitor present. After another 2 h at 37 °C, the cells were washed with a heparin-containing solution to effectively remove polyplexes still present in the medium and, in particular, those attached to the cell surface (*cf.* Figure 2). The cells were subsequently incubated for 48 h in the absence of the inhibitor, after which the transfection efficiency was determined, as described in Materials and Methods. As shown in Figure 7, relative to the control, both blebbistatin and jasplakinolide inhibited transfection efficiency in a concentration-dependent manner. Thus depending on the nature of the inhibitor, PEI-mediated transfection efficiency was inhibited between 50 and 90%, implying that at the present conditions at least 50% of the overall transfection efficiency is contributed by initial processing of the PEI polyplexes along filopodia and fibers. At similar conditions, lipoplex-mediated transfection was inhibited between 40 and 70% (not shown).

Whether filopodia-mediated transport is linked to a specific pathway of entry of the polyplexes, or once arrived at the cell body, polyplexes may redistribute for cellular entry *via* multiple endocytic pathways, remains to be determined.

CONCLUSIONS

In the present work we have shown that nanocarriers, that is, poly- and lipoplexes, do not necessarily randomly attach at the cell surface by simple electrostatic interactions, preceding their entry into the cell. Rather, we observed that syndecans, localized at filopodia and retraction fibers, can be highly instrumental in guiding such particles to the cell surface. Specifically, we demonstrate here that the binding of the nanocarriers to syndecans triggers actin retrograde flow, which carries them along filopodia to the cell body. This filopodia-mediated processing occurs along distinct mechanisms, including the surfing of polyplexes along the filopodia, after initial binding to and subsequent clustering of syndecans, which presumably relates to multivalent interactions between syndecans and the charged nanocarriers. Alternatively, the polyplexes may reach the cell body as a result of retraction of the filopodia and fibers, a mechanism that closely resembles that recently proposed for bacteria.[24] What determines filopodia to either support ligand surfing or show retraction is largely unknown. Also there may exist multiple populations of filopodia, each performing a specific function. Possibly, the filopodia that are in contact with the extracellular substratum support only surfing, while the filopodia that are oriented "loose" in the extracellular space can be involved in both surfing and retraction.

Interestingly, syndecan dynamics was a key factor in processing of the polyplexes along the filopodia, and the link to actin retrograde flow *via* a myosin II driven mechanism, as reported before for the surfing of other ligands and viruses along filopodia as well as their retraction,[19,28] seems apparent. Interfering with the latter process or with the state of actin polymerization, clearly affected the lateral dynamics of the transmembrane actin-interacting syndecan receptors. Thus at such conditions, triggered upon treatment of the cells with blebbistatin or jasplakinolide, the polyplexes could still bind to the filopodia, but at both conditions lateral movement of the receptors is impeded and hence subsequent recruitment and clustering of syndecan receptors was strongly diminished or abolished. As a result, the remaining syndecans failed to stabilize

the binding of polyplexes and as a consequence the polyplexes dissociated from their binding sites, implying a relatively weak interaction as such, following initial binding.

Evidently, given conditions as described in the present work, filopodia-mediated attachment and processing of PEI polyplexes can play a major role in polyplex-mediated transfection as the latter is inhibited by 50−90% when the processing of polyplexes along filopodia is inhibited . The exclusiveness of this mechanism remains to be determined, particularly since changes of filopodia expression by modulating cell culture conditions do not seemingly affect viral infection activity.[18] Furthermore, whether multiple populations of filopodia, next to retraction fibers, are involved in this process, each performing its specific function,[21] cannot be ruled out either, and also requires further investigations. Nevertheless, knowledge about the early binding and processing of polyplexes to the filopodia may be of direct relevance to clarifying filopodia mediated processing of viruses and bacteria, and further investigation of this mechanism will aid in understanding cellular infection by viruses and pathogenic bacteria.

MATERIALS AND METHODS

Reagents and Antibodies. Linear polyethylenimine (LPEI) (average MW = 22 kDa) was purchased from PolyPlus-transfection (Illkirch, France), FITC-labeled poly-L-lysine (FITC-PLL) was from Sigma (Zwijndrecht, The Netherlands). Cytochalasin D and sodium azide were purchased from Sigma (Zwijndrecht, The Netherlands). Blebbistatin was obtained from Toronto Research Chemicals, while jasplakinolide was from Calbiochem. Heparinase II was purchased from Sigma (Zwijndrecht, The Netherlands).

Cells. HeLa cells were maintained in 25 cm^2 Coster Flasks in Dulbecco's Modified Eagle Medium nutrient mixture F-12 (DMEM/F-12, Gibco, The Netherlands), containing 10% (v/v) fetal calf serum (FCS), 2 mM L-glutamine (Gibco, The Netherlands), 100units/mL penicillin (Invitrogen) and 100ug/mL streptomycin (Invitrogen) at 37 °C and 5% CO_2. hCMEC/D3 (Human cerebral microvessel endothelial cells) were maintained in 25 cm^2 flasks precoated with 100ug/mL rat tail collagen type-1 (BD Biosciences, Franklin Lakes, NJ) in endothelial basal medium-2 (EBM-2; Lonza Group, Basel, Switzerland), supplemented with EGM-2-MV bullet kit (Lonza) containing vascular endothelial growth factor, R^3-insulin-like growth factor-1, human epidermal growth factor, human fibroblast growth factor-basic, hydrocortisone, 2.5% fetal bovine serum, and 100 ug/mL penicillin/streptomycin.

HEK293 cells were cultured in 25 cm^2 flasks in Dulbecco's Modified Eagle Medium (Gibco, The Netherlands), supplemented with 10% FCS, 100ug/mL penicillin/streptomycin, and 2 mM L-glutamine (Gibco, The Netherlands).

PC3 prostate cancer cells were maintained in Ham's F-12 nutrient mixture, Kaighn's modifications (Sigma Chemical Co.), supplemented with 10% FCS.

PNT2 cells were cultured in 25 cm^2 flasks in Dulbecco's Modified Eagle Medium (Gibco, The Netherlands), supplemented with 10% FCS, 100ug/mL penicillin/streptomycin. Cells were passaged every third day.

Plasmids. Plasmids DNA were obtained from the following sources: pEGFP-N1 was obtained from Clontech (USA), pSDC1-GFP (syndecan-1), and pSDC2-RFP (syndecan-2) were kindly provided by Dr. Yves Durocher (National Research Council (NRC) Canada). Plasmid DNA was amplified from *E. coli*. using Sigma Aldrich GenElute HP Plasmid Mini/Midiprep kits (Sigma-Aldrich), following the manufacturer's protocol.

Transfection with Lipoplexes and Polyplexes. Lipoplexes were made with Lipofectamine 2000 (Invitrogen) and polyplexes were made with linear polyethyleneimine (LPEI, Polyplus-transfection), mixed with plasmid DNA, according to the manufacturers' protocols. LPEI polyplexes were prepared at an N/P ratio of 5. Size and zeta potential measurements were measured in 0.15 M NaCl using a Zetasizer Nano (Malvern Instruments Ltd.) LF2000 lipoplexes: Average diameter 1424 nm, −34.7 mV. LPEI polyplexes: average diameter 740 nm, 22.7 mV.

For transfection studies, HeLa cells were plated one day before transfection in 12 wells plates at 1.5×10^5 cells/well. The next day, the cells were washed with transfection medium, and subsequently incubated in 0.5 mL/well of the same medium. Lipo/polyplexes containing 1 μg of pEGFP-N1in 200ul of HBSS buffer were added per well and incubated at 37 °C. After an incubation of 2 h, the medium was removed and fresh culture medium was added, which was repeated after 24 h. The transfection efficiency was measured after 48 h, using FACS-analysis (Elite, Coulter 10 000 events λ_{ex}. 488 nm/λ_{em}. 530 nm).

For confocal microscopy and live cell imaging, lipo/polyplexes were fluorescently labeled by using Cy3-labeled pDNA (Mirus, MA). Polyplexes per se were labeled by using FITC-PLL, as previously described.[8] Briefly, 3.6 μL of 1 mM FITC-PLL was mixed with 2 μg of plasmid DNA and incubated for 15 min at room temperature. Then PEI polymers were added, and the mixture was further incubated at room temperature for 20 min to allow assembly of the fluorescently tagged complexes.

In the inhibitor studies, the cells were preincubated with the specified inhibitor for 30 min, unless stated otherwise, followed by addition of the polyplexes with the inhibitors still present.

Confocal Microscopy. Confocal microscopy was performed as described before.[8] Briefly, HeLa cells were plated one day before the experiment at 1.5×10^5cells/mL on glass coverslips in a 12-wells plate. For colocalization studies with syndecans, cells transiently expressing SDC1-GFP or SDC2-RFP were used. Briefly, HeLa cells were plated at 1×10^5cells/mL on glass coverslips two days prior to the experiment. On the following day cells were transfected with either SDC1-GFP or SDC2-RFP using Lipofectamine2000 as transfection reagent. On the day of the experiment cells were incubated with fluorescently labeled polyplexes, as indicated. Afterward, cells were washed three times with PBS, and fixed with 4% *para*-formaldehyde (PFA) in PBS for 20 min. PFA was subsequently quenched with 0.1 M glycin in PBS for 20 min. For actin staining, cells were permeabilized with 0.2% triton X-100 for 2 min and incubated with alexa 488 or alexa 633 labeled phalloidin for 30 min at 37 °C in a humid chamber. Cells were then washed three times with PBS and finally the coverslips were mounted on glass slides using Dako mounting medium (Dako, Carpinteria, USA). A Leica TCS SP2 confocal microscope (Leica Microsystem, Germany) was used to visualize the samples, using a 63× oil immersion lens. Images were further analyzed using ImageJ (NIH).

Live Cell Imaging. For live cell imaging, the cells were plated on glass bottomed 2-wells plates (Lab-Tek Chambered Coverglass, Thermo Fisher Scientific, Denmark) two days prior to the experiment at 1.8×10^5 cell/well). The next day the cells were transfected with the SDC1-GFP and SDC2-RFP plasmids, using LF2000. On the day of the experiment the syndecan expressing HeLa cells were preincubated with inhibitors for 30 min, as indicated, or placed directly in a Solamere Spinning Disk Confocal Microscope (based on a Leica DM IRE2 Inverted microscope, Leica Microsystems, Germany, Solamere, Salt Lake City, USA) equipped with a temperature/CO_2 controlled cabinet and an automated stage. Cells expressing syndecans were selected for imaging prior to the addition of lipo/polyplexes. After addition of lipo/polyplexes image acquisition was directly started using *InVivo* software (Media Cybernetics, Inc., Bethesda, MD). Images were further analyzed using ImageJ (NIH) and Imaris (Bitplane AG, Switzerland).

Scanning Electron Microscopy. Cells were incubated with the polyplexes for 90 min, washed three times with PBS, and fixed overnight with 2% glutaraldehyde in 0.1 M sodium cacodylate pH = 7.4 at 4 °C. Subsequently, samples were washed three times with 0.1 M sodium cacodylate pH = 7.4 and PBS, and post fixed with 1% osmium tetroxide in 0.1 M cacodylate buffer for 1 h at room temperature, and rinsed with distilled water. The samples were then dehydrated with a gradient of 30, 50, 70% ethanol for 15 min each, followed by three times with 100% ethanol for 30 min each, and dried by critical point drying (CPD) with CO_2. The dried samples were then coated with 5 nm Pd/Au using Leica EM SCD050 sputtercoater and analyzed with a JEOL 6301F (JEOL, Japan) scanning electron microscope, operating at 3 kV.

Conflict of Interest: The authors declare no competing financial interest.

Acknowledgment. Microscopy imaging was performed at the UMCG Imaging Center (UMIC), supported by The Netherlands Organisation for Health Research and Development (ZonMW grant 40-00506-98-9021).

Supporting Information Available: Supporting Figure S1 and 10 movies as described in the text. This material is available free of charge *via* the Internet at http://pubs.acs.org.

REFERENCES AND NOTES

1. Kamimura, K.; Suda, T.; Zhang, G.; Liu, D. Advances in gene delivery systems. *Pharm. Med.* **2011**, *25*, 293–306.
2. Boussif, O.; Lezoualc'h, F.; Zanta, M. A.; Mergny, M. D.; Scherman, D.; Demeneix, B.; Behr, J. P. A versatile vector for gene and oligonucleotide transfer into cells in culture and *in vivo*: Polyethylenimine. *Proc. Natl. Acad. Sci. U.S.A.* **1995**, *92*, 7297–7301.
3. Simoes, S.; Slepushkin, V.; Pires, P.; Gaspar, R.; de Lima, M. P.; Duzgunes, N. Mechanisms of gene transfer mediated by lipoplexes associated with targeting ligands or pH-sensitive peptides. *Gene Ther.* **1999**, *6*, 1798–1807.
4. Elouahabi, A.; Ruysschaert, J. M. Formation and intracellular trafficking of lipoplexes and polyplexes. *Mol. Ther.* **2005**, *11*, 336–347.
5. Zuhorn, I. S.; Kalicharan, R.; Hoekstra, D. Lipoplex-mediated transfection of mammalian cells occurs through the cholesterol-dependent clathrin-mediated pathway of endocytosis. *J. Biol. Chem.* **2002**, *277*, 18021–18028.
6. Rejman, J.; Oberle, V.; Zuhorn, I. S.; Hoekstra, D. Size-dependent internalization of particles *via* the pathways of clathrin- and caveolae-mediated endocytosis. *Biochem. J.* **2004**, *377*, 159–169.
7. Rejman, J.; Bragonzi, A.; Conese, M. Role of clathrin- and caveolae-mediated endocytosis in gene transfer mediated by lipo- and polyplexes. *Mol. Ther.* **2005**, *12*, 468–474.
8. ur Rehman, Z.; Hoekstra, D.; Zuhorn, I. S. Protein kinase A inhibition modulates the intracellular routing of gene delivery vehicles in HeLa cells, leading to productive transfection. *J. Controlled Release* **2011**, *156*, 76–84.
9. Zuhorn, I. S.; Kalicharan, D.; Robillard, G. T.; Hoekstra, D. Adhesion receptors mediate efficient non-viral gene delivery. *Mol. Ther.* **2007**, *15*, 946–953.
10. Kopatz, I.; Remy, J. S.; Behr, J. P. A model for non-viral gene delivery: Through syndecan adhesion molecules and powered by actin. *J. Gene Med.* **2004**, *6*, 769–776.
11. Ruponen, M.; Ronkko, S.; Honkakoski, P.; Pelkonen, J.; Tammi, M.; Urtti, A. Extracellular glycosaminoglycans modify cellular trafficking of lipoplexes and polyplexes. *J. Biol. Chem.* **2001**, *276*, 33875–33880.
12. Giroglou, T.; Florin, L.; Schafer, F.; Streeck, R. E.; Sapp, M. Human papillomavirus infection requires cell surface heparan sulfate. *J. Virol.* **2001**, *75*, 1565–1570.
13. Spillmann, D. Heparan sulfate: Anchor for viral intruders? *Biochimie* **2001**, *83*, 811–817.
14. Barth, H.; Schafer, C.; Adah, M. I.; Zhang, F.; Linhardt, R. J.; Toyoda, H.; Kinoshita-Toyoda, A.; Toida, T.; Van Kuppevelt, T. H.; Depla, E.; *et al.* Cellular binding of hepatitis C virus envelope glycoprotein E2 requires cell surface heparan sulfate. *J. Biol. Chem.* **2003**, *278*, 41003–41012.
15. Bacsa, S.; Karasneh, G.; Dosa, S.; Liu, J.; Valyi-Nagy, T.; Shukla, D. Syndecan-1 and syndecan-2 play key roles in herpes simplex virus type-1 infection. *J. Gen. Virol.* **2011**, *92*, 733–743.
16. Menozzi, F. D.; Reddy, V. M.; Cayet, D.; Raze, D.; Debrie, A. S.; Dehouck, M. P.; Cecchelli, R.; Locht, C. Mycobacterium tuberculosis heparin-binding haemagglutinin adhesin (HBHA) triggers receptor-mediated transcytosis without altering the integrity of tight junctions. *Microbes Infect.* **2006**, *8*, 1–9.
17. Smith, M. F., Jr; Novotny, J.; Carl, V. S.; Comeau, L. D. Helicobacter pylori and toll-like receptor agonists induce syndecan-4 expression in an NF-kappaB-dependent manner. *Glycobiology* **2006**, *16*, 221–229.
18. Schelhaas, M.; Ewers, H.; Rajamaki, M. L.; Day, P. M.; Schiller, J. T.; Helenius, A. Human papillomavirus type 16 entry: Retrograde cell surface transport along actin-rich protrusions. *PLoS Pathog.* **2008**, *4*, e1000148.
19. Lehmann, M. J.; Sherer, N. M.; Marks, C. B.; Pypaert, M.; Mothes, W. Actin- and myosin-driven movement of viruses along filopodia precedes their entry into cells. *J. Cell Biol.* **2005**, *170*, 317–325.
20. Paris, S.; Burlacu, A.; Durocher, Y. Opposing roles of syndecan-1 and syndecan-2 in polyethyleneimine-mediated gene delivery. *J. Biol. Chem.* **2008**, *283*, 7697–7704.
21. Mattila, P. K.; Lappalainen, P. Filopodia: molecular architecture and cellular functions. *Nat. Rev. Mol. Cell Biol.* **2008**, *9*, 446–454.
22. Sherer, N. M.; Lehmann, M. J.; Jimenez-Soto, L. F.; Horensavitz, C.; Pypaert, M.; Mothes, W. Retroviruses can establish filopodial bridges for efficient cell-to-cell transmission. *Nat. Cell Biol.* **2007**, *9*, 310–315.
23. Oh, M. J.; Akhtar, J.; Desai, P.; Shukla, D. A role for heparan sulfate in viral surfing. *Biochem. Biophys. Res. Commun.* **2010**, *391*, 176–181.
24. Romero, S.; Grompone, G.; Carayol, N.; Mounier, J.; Guadagnini, S.; Prevost, M. C.; Sansonetti, P. J.; Van Nhieu, G. T. ATP-mediated Erk1/2 activation stimulates bacterial capture by filopodia, which precedes Shigella invasion of epithelial cells. *Cell. Host Microbe* **2011**, *9*, 508–519.
25. Mislick, K. A.; Baldeschwieler, J. D. Evidence for the role of proteoglycans in cation-mediated gene transfer. *Proc. Natl. Acad. Sci. U.S.A.* **1996**, *93*, 12349–12354.
26. Ernst, S.; Langer, R.; Cooney, C. L.; Sasisekharan, R. Enzymatic degradation of glycosaminoglycans. *Crit. Rev. Biochem. Mol. Biol.* **1995**, *30*, 387–444.
27. Vercauteren, D.; Piest, M.; van der Aa, L. J.; Al Soraj, M.; Jones, A. T.; Engbersen, J. F.; De Smedt, S. C.; Braeckmans, K. Flotillin-dependent endocytosis and a phagocytosis-like mechanism for cellular internalization of disulfide-based poly(amido amine)/DNA polyplexes. *Biomaterials* **2011**, *32*, 3072–3084.
28. Lidke, D. S.; Lidke, K. A.; Rieger, B.; Jovin, T. M.; Arndt-Jovin, D. J. Reaching out for signals: filopodia sense EGF and respond by directed retrograde transport of activated receptors. *J. Cell Biol.* **2005**, *170*, 619–626.
29. Rustom, A.; Saffrich, R.; Markovic, I.; Walther, P.; Gerdes, H. H. Nanotubular highways for intercellular organelle transport. *Science* **2004**, *303*, 1007–1010.
30. Onfelt, B.; Nedvetzki, S.; Yanagi, K.; Davis, D. M. Cutting edge: Membrane nanotubes connect immune cells. *J. Immunol.* **2004**, *173*, 1511–1513.
31. Onfelt, B.; Purbhoo, M. A.; Nedvetzki, S.; Sowinski, S.; Davis, D. M. Long-distance calls between cells connected by tunneling nanotubules. *Sci. STKE* **2005**, *2005*, pe55.
32. Sherer, N. M.; Mothes, W. Cytonemes and tunneling nanotubules in cell-cell communication and viral pathogenesis. *Trends Cell Biol.* **2008**, *18*, 414–420.
33. Sowinski, S.; Jolly, C.; Berninghausen, O.; Purbhoo, M. A.; Chauveau, A.; Kohler, K.; Oddos, S.; Eissmann, P.; Brodsky, F. M.; Hopkins, C.; *et al.* Membrane nanotubes physically connect T cells over long distances presenting a novel route for HIV-1 transmission. *Nat. Cell Biol.* **2008**, *10*, 211–219.

34. Hope, T. J. Bridging efficient viral infection. *Nat. Cell Biol.* **2007**, *9*, 243–244.
35. Gallo, G.; Letourneau, P. C. Regulation of growth cone actin filaments by guidance cues. *J. Neurobiol.* **2004**, *58*, 92–102.
36. Freissler, E.; Meyer auf der Heyde, A.; David, G.; Meyer, T. F.; Dehio, C. Syndecan-1 and syndecan-4 can mediate the invasion of OpaHSPG-expressing Neisseria gonorrhoeae into epithelial cells. *Cell. Microbiol.* **2000**, *2*, 69–82.
37. Lin, C. H.; Espreafico, E. M.; Mooseker, M. S.; Forscher, P. Myosin drives retrograde F-actin flow in neuronal growth cones. *Neuron* **1996**, *16*, 769–782.
38. Welch, M. D.; Mallavarapu, A.; Rosenblatt, J.; Mitchison, T. J. Actin dynamics *in vivo*. *Curr. Opin. Cell Biol.* **1997**, *9*, 54–61.
39. Straight, A. F.; Cheung, A.; Limouze, J.; Chen, I.; Westwood, N. J.; Sellers, J. R.; Mitchison, T. J. Dissecting temporal and spatial control of cytokinesis with a myosin II Inhibitor. *Science* **2003**, *299*, 1743–1747.
40. Mao, Y. S.; Yamaga, M.; Zhu, X.; Wei, Y.; Sun, H. Q.; Wang, J.; Yun, M.; Wang, Y.; Di Paolo, G.; Bennett, M.; *et al*. Essential and unique roles of PIP5K-γ and -α in Fcγ receptor-mediated phagocytosis. *J. Cell Biol.* **2009**, *184*, 281–296.